ceramics

MDPI

Article

Zero-Temperature Coefficient of Resonant Frequency in $[(Mg_{0.6}Zn_{0.4})_{0.95}Co_{0.05}]_{1.02}TiO_{3.02}$-$Ca_{0.6}(La_{0.9}Y_{0.1})_{0.2667}TiO_3$ Ultra-Low-Loss Composite Dielectrics

Yuan-Bin Chen * and Jie Peng *

School of Electronics and Electrical Engineering, Zhaoqing University, Zhaoqing 526061, China
* Correspondence: n2890103@outlook.com (Y.-B.C.); kit.j.peng@gmail.com (J.P.)

Abstract: Investigating the microwave dielectric properties of ceramics prepared through the conventional solid-state route, such as $x[(Mg_{0.6}Zn_{0.4})_{0.95}Co_{0.05}]_{1.02}TiO_{3.02}$-$(1-x)Ca_{0.6}(La_{0.9}Y_{0.1})_{0.2667}TiO_3$, reveals notable characteristics. $[(Mg_{0.6}Zn_{0.4})_{0.95}Co_{0.05}]_{1.02}TiO_{3.02}$ shows a permittivity (ε_r) of approximately 20, a high quality factor ($Q \times f$) ranging between 250,000 and 560,000 GHz, and a temperature coefficient of resonant frequency (τ_f) of approximately −65 ppm/°C. To enhance the temperature stability, $Ca_{0.6}(La_{0.9}Y_{0.1})_{0.2667}TiO_3$ featuring a τ_f value of +374 ppm/°C was incorporated into the $[(Mg_{0.6}Zn_{0.4})_{0.95}Co_{0.05}]_{1.02}TiO_{3.02}$ composition. τ_f demonstrated an increase with rising $Ca_{0.6}(La_{0.9}Y_{0.1})_{0.2667}TiO_3$ content, reaching zero at x = 0.95. A ceramic composition of $0.95[(Mg_{0.6}Zn_{0.4})_{0.95}Co_{0.05}]_{1.02}TiO_{3.02}$-$0.05Ca_{0.6}(La_{0.9}Y_{0.1})_{0.2667}TiO_3$, incorporating 3wt.% $BaCu(B_2O_5)$ as sintering aids, exhibited outstanding microwave dielectric properties: ε_r~22.5, Q × f~195,000 (at 9 GHz), and τ_f~0.1ppm/°C, with a sintering temperature at 950 °C. This material is proposed as a prospective candidate for 6G band components and GPS antennas.

Keywords: $[(Mg_{0.6}Zn_{0.4})_{0.95}Co_{0.05}]_{1.02}TiO_{3.02}$; $Ca_{0.6}(La_{0.9}Y_{0.1})_{0.2667}TiO_3$; microwave dielectric properties; temperature coefficient of resonant frequency

check for updates

Citation: Chen, Y.-B.; Peng, J. Zero-Temperature Coefficient of Resonant Frequency in $[(Mg_{0.6}Zn_{0.4})_{0.95}Co_{0.05}]_{1.02}TiO_{3.02}$-$Ca_{0.6}(La_{0.9}Y_{0.1})_{0.2667}TiO_3$ Ultra-Low-Loss Composite Dielectrics. *Ceramics* **2024**, *7*, 466–477. https://doi.org/10.3390/ceramics7020030

Academic Editors: Dawei Wang and Fayaz Hussain

Received: 15 January 2024
Revised: 18 March 2024
Accepted: 22 March 2024
Published: 26 March 2024

Copyright: © 2024 by the authors. Licensee MDPI, Basel, Switzerland. This article is an open access article distributed under the terms and conditions of the Creative Commons Attribution (CC BY) license (https://creativecommons.org/licenses/by/4.0/).

1. Introduction

The distinct electrical properties of ceramic dielectric resonators (DRs) have spurred a revolution in the wireless communications industry by minimizing the dimensions and cost of oscillator and filter components within the microwave circuit [1–3]. The integration of DRs enables the downsizing of microwave components, with requirements including a low dielectric loss, high permittivity, and a closee-zero τ_f [4–8]. The product of the quality factor (Q) and the frequency (f), denoted as Q × f, exhibits an inverse relationship with the dielectric loss tangent (tanδ) in dielectric materials. Specifically, a higher value of Q × f signifies a lower dielectric loss, which is particularly crucial for the efficiency of ceramics used in microwave dielectrics [9]. These materials have become the preferred choice for 6G communications owing to their exceptional low-loss properties [10–12].

$MgTiO_3$-based ceramics, known for their low dielectric loss, have been the subject of intensive research. The $MgTiO_3$-$CaTiO_3$ ceramic, composed of a blend of $MgTiO_3$ (ε_r approximately 17, Q × f approximately 160,000 (at 9 GHz), and τ_f approximately −50 ppm/°C) [13] and $CaTiO_3$ (ε_r~170, Q × f~3600 (at 7 GHz), and τ_f~800 ppm/°C) [14], has been utilized in dielectric resonators and patch antennas. A ceramic composition of 0.95 $MgTiO_3$-0.05$CaTiO_3$ exhibits ε_r~21, a Q × f~56,000 (at 7 GHz), and a zero τ_f value, but necessitates high sintering temperatures of 1400~1450 °C [15]. In industrial settings, there is a pressing need to reduce the sintering temperature in order to enhance energy efficiency, lower production costs, and mitigate potential adverse effects on the material properties during the fabrication process [16–19]. Given the close similarity in ionic radii between Zn^{2+} (0.083 nm) and Mg^{2+} (0.078 nm), the strategic substitution of Zn^{2+}

ions with Mg^{2+} ions emerges as a viable approach for crafting (Mg, Zn)TiO_3 compositions. The incorporation of Zn into $MgTiO_3$ to create a solid solution, (Mg, Zn)TiO_3, has proven advantageous not only because it maintains the structural integrity but also because it reduces the required sintering temperature. This not only streamlines the manufacturing process but also holds promise for optimizing material properties in practical industrial applications. For instance, $(Mg_{0.7}Zn_{0.3})TiO_3$, sintered at 1200 °C, exhibits ε_r~19.8, Q × f~142,000 GHz, and τ_f~−66 ppm/°C [20]. Additionally, incorporating Co into $(Mg_{0.7}Zn_{0.3})$, as seen in $(Mg_{0.7}Zn_{0.3})_{0.95}Co_{0.05}TiO_3$, results in excellent dielectric properties, with ε_r~20, Q × f~163,560 GHz, and τ_f~−65 ppm/°C, even when sintered at a relatively low temperature of 1200 °C [21]. Non-stoichiometric ceramic $Mg_{1+\delta}$ $TiO_{3+\delta}$ compositions were initially reported by Huang [22]. The Q × f value exhibited a nonlinear variation, reaching a peak of approximately 357,600 GHz when δ reached 0.02, beyond which it exhibited a decline. This noteworthy peak in the Q × f value is attributed to the distinct $MgTiO_3$ phase, underscoring the influence of non-stoichiometry on the microwave properties of the ceramic material. The exploration of these non-stoichiometric variations holds the potential for tailoring and optimizing microwave characteristics in diverse applications.

In this paper, we explore the substitution of Zn^{2+} and Co^{2+} ions for Mg^{2+} ions, resulting in the formation of $[(Mg_{0.6}Zn_{0.4})_{0.95}Co_{0.05}]_{1.02}TiO_{3.02}$ (MZCT). The ionic radius of Mg (0.78 Å) closely resembles that of Zn^{2+} (0.83 Å) and Co^{2+} (0.82 Å). Consequently, the substitution greatly enhanced the Q × f value, which establishes it as a highly dependable method for producing materials with consistent dielectric properties. The dielectric properties in the microwave applications were assessed through the analysis of X-ray diffraction (XRD) patterns, densification, and microstructures.

We investigated the partial substitution of Y^{3+} for La^{3+} in $Ca_{0.6}La_{0.2667}TiO_3$ ceramics. This substitution is viable due to the smaller ionic radius of Y^{3+} (0.106 Å) compared to that of La^{3+} (0.122 Å), allowing for the formation of $Ca_{0.6}(La_{0.9}Y_{0.1})_{0.2667}TiO_3$ (CLYT). A solid-state synthesis method was employed in this study. Examining the correlations between the surface morphology and quantity of CLYT ceramics sintered at 1350 °C revealed the following properties: ε_r = 111, Q × f = 23,100 (GHz), and τf = 374.6 ppm/°C. The formation of $BaCu(B_2O_5)$ (BCB) was observed at 700 °C, with subsequent melting occurring above 850 °C [23–25]. Due to its low melting temperature and advanced microwave dielectric properties, BCB proved effective as a sintering aid for microwave dielectric materials [22].

In this work, BCB powder was employed to effectively reduce the sintering temperature during the fabrication of the xMZCT-(1−x)CLYT ceramics. The impact of BCB on the microwave dielectric properties of the ceramics was investigated.

2. Experiments

MZCT was synthesized using the solid-state mixed oxide route, employing high-purity oxide powders (>99.9%) such as $MgCO_3{\cdot}0.2708H_2O$ as starting materials. The decomposition reaction of $MgCO_3{\cdot}0.2708H_2O$ at temperatures between 600 and 700 °C for 5 h can be represented as follows [26]:

$$MgCO_3{\cdot}0.2708H_2O \rightarrow MgO + CO_2 + xH_2O$$

The ceramic preparation process commenced with an initial firing at 650 °C to eliminate moisture content and ensure a stable starting point. MZCT ceramics were fabricated through a conventional solid-state reaction utilizing high-purity oxide powders (MgO, ZnO, CoO, and TiO_2). The raw materials were precisely weighed and subjected to a thorough mixing process through ball milling with agate media in distilled water for an extensive period of 24 h. Following meticulous mixing, resulting mixtures underwent a drying phase before being carefully calcined at a temperature of 1000 °C for 4 h.

Samples of CLYT ceramics were fabricated through a conventional solid-state reaction utilizing high-purity oxide powders ($CaCO_3$, La_2O_3, Y_2O_3, and TiO_2). The process involved mixing, milling for 24 h, drying, and grinding, followed by calcination at 1000 °C for 2 h. XRD analyses were employed to identify the crystal phases of the calcined powders. For

the synthesis of BCB, $BaCO_3$ (>99%), CuO (>99%), and B_2O_3 (>99%) were mixed for 4 h in a nylon jar with zirconia balls and then dried and calcined at 700 °C for 3 h. Subsequently, xMZCT-(1−x)CLYT powders were dry-mixed with an agate mortar and pestle before being wet-mixed using distilled water for 12 h. To facilitate the formation of well-structured ceramic samples, a finely powdered mixture was prepared, incorporating 3 wt% of a 10 wt% of an aqueous solution of polyvinyl alcohol (PVA 500, Showa, Japan) solution as a binder. This mixture was meticulously compressed into pellets, with each one measuring 1.1 cm in diameter and 0.5 cm in thickness, utilizing a pressure of 200 MPa to ensure a compact and uniform structure.

Following pelletization, the specimens underwent a sintering process in ambient air, for a duration of 4 h at temperatures ranging from 900 to 1000 °C. Throughout this thermal treatment, both the heating and cooling rates were carefully controlled at 10 °C/min to prevent thermal stress and ensure a gradual transformation. To assess the structural evolution, an X-ray diffraction pattern analysis was employed. This analytical technique was applied to identify the crystalline phases present in both the calcined powder and the sintered ceramics, providing valuable insights into the structural changes and the formation of desired phases during the manufacturing process. Scanning electron microscopy (SEM, Philips XL-40FEG, Eindhoven, The Netherlands) was used in the microstructure analysis of the sintered surface. Additionally, dispersive spectroscopy (EDS) was utilized to identify the presence of any second phases. The Archimedes method was used to measure the bulk densities of the sintered pellets. The Hakki–Coleman [27] dielectric resonator method, adapted and refined by Courtney [28], was applied to determine the permittivity and the quality factor value at the microwave frequencies under both TE011 and TE01 modes.

For measurement purposes, the dielectric resonator was meticulously placed between two brass plates, establishing a reliable and controlled environment to assess the microwave properties with precision. A comprehensive measurement system that utilized the synergistic capabilities of an HP8350B sweep oscillator and an HP8757D network analyzer for precision analysis was employed. The test set was positioned atop a thermostat, spanning a temperature spectrum in the range of 25 to 80 °C. The τ_f value can be calculated using Equation (1).

$$\tau_f = \frac{f_{80} - f_{25}}{f_{25}(80 - 25)} \times 10^6 (\text{ppm}/^\circ\text{C}) \quad (1)$$

where f_{80} and f_{25} represent the resonant frequencies at 80 and 25 °C, respectively.

3. Results and Discussion

Figure 1 depicts the X-ray diffraction (XRD) pattern of 0.95MZCT-0.05CLYT, augmented with a 3wt.% BCB dopant, recorded at room temperature. The crystal structures of MZCT and CLYT were revealed to be rhombohedral (ICDD-PDF #01-073-7752) and orthorhombic (ICDD-PDF #00-022-0153), respectively. Remarkably, the XRD patterns reveal the persistent presence of the MZCT phase in these specimens, exhibiting negligible alternations with varying sintering temperatures within the range of 900–1000 °C. The XRD patterns affirm the dominance of MZCT as the major crystalline phase, accompanied by a minor phase of CLYT. The inability to achieve a solid solution in the xMZCT-(1−x)CLYT ceramic system is attributed to inherent structural disparities. Notably, the XRD patterns of the 0.95MZCT-0.05CLYT ceramic exhibit minimal fluctuations across the sintering temperature spectrum of 900–1000 °C. In Figure 2, SEM images of the 0.95MZCT-0.05CLYT ceramic, doped with 3wt.% BCB and subjected to various sintering temperatures, are presented. At 900 °C, porous microstructures are evident in the grains. Grain growth is initiated at 950 °C and significantly escalates at 975 °C. Beyond 975 °C, inhomogeneous grain growth becomes apparent, potentially impacting the microwave dielectric properties of the ceramics.

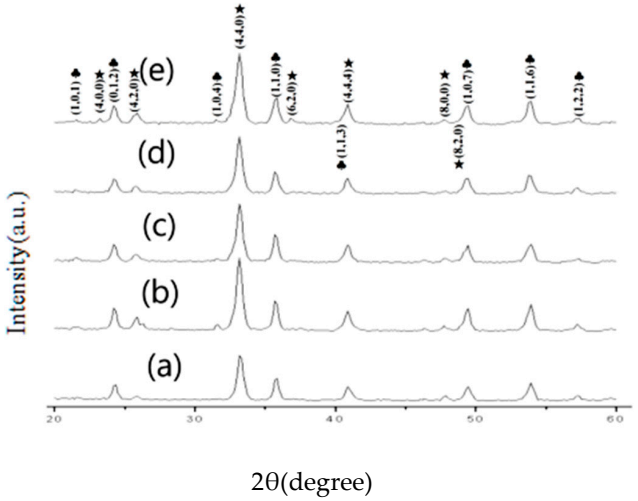

Figure 1. X-ray diffraction patterns of 0.95MZCT-0.05CLYT ceramics doped with 3wt.% BCB and sintered at various temperatures for 4 h: (**a**) 900 °C, (**b**) 925 °C, (**c**) 950 °C, (**d**) 975 °C, and (**e**) 1000 °C (♣: MZCT; ★: CLYT).

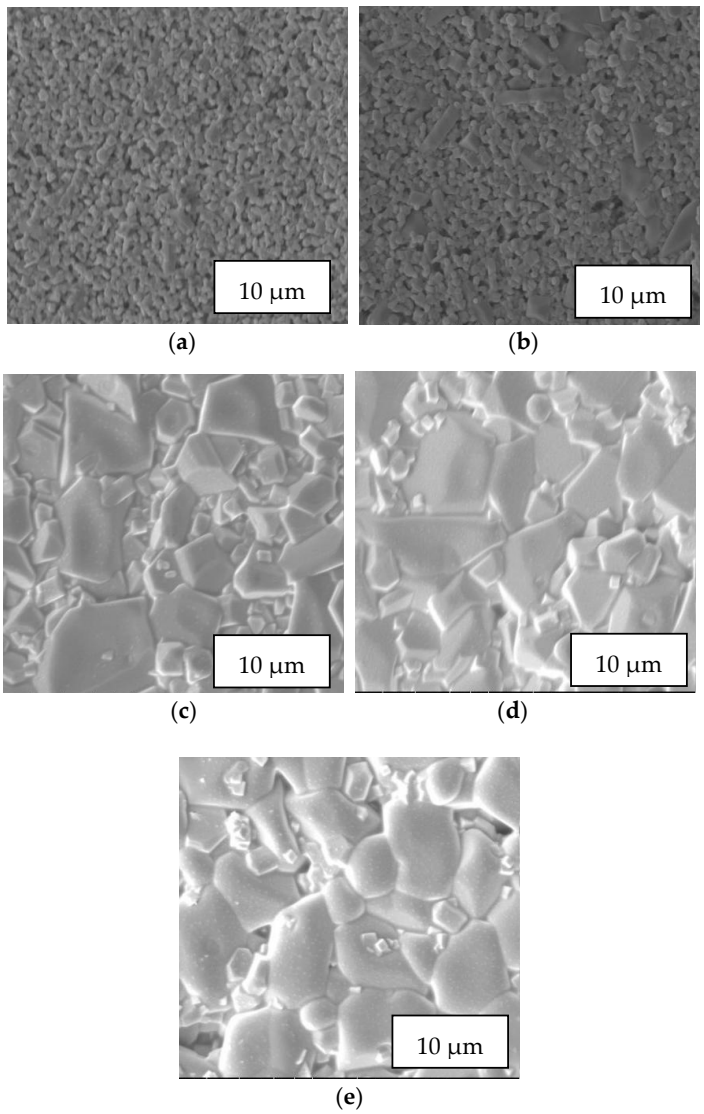

Figure 2. SEM micrographs of 0.95MZCT-0.05CLYT ceramics doped with 3wt.% BCB and sintered at (**a**) 900, (**b**) 925, (**c**) 950, (**d**) 975, and (**e**) 1000 °C.

Energy-dispersive X-ray (EDX) analysis, complemented by SEM, was employed to discern each individual grain in the 0.95MZCT-0.05CLYT ceramics sintered at 950 °C, and the results, along with the corresponding spots A–B, are presented in Figure 3. The grain morphology of the well-developed 0.95MZCT-0.05CLYT ceramics can be classified into two types: the larger grains (spot A), indicated as the Mg–Ti phase, were confirmed to be MZCT, while the smaller cubic-shaped grains (spot B) were identified as CLYT. The EDX findings align with the XRD results obtained from the 0.95MZCT-0.05CLYT ceramics. In contrast to the pure MZCT, CLYT exhibits a lower sintering temperature. This discrepancy arises from the smaller grain size of CLYT compared to that of MZCT, and the incorporation of CLYT into MZCT contributes to the improved densification of the ceramics. Details of the EDX data for spots A-B are shown in Table 1, offering insights into the elemental composition at specific regions. The well-developed grain morphology shows the distinctive characteristics of the dual-phase ceramics.

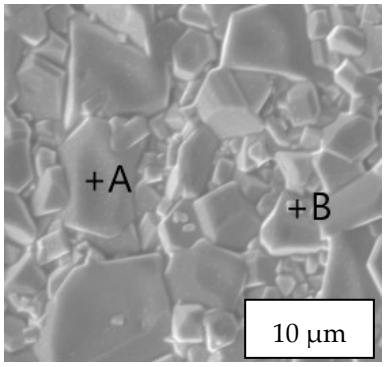

Figure 3. The marks of SEM for the 0.95MZCT-0.05CLYT ceramics doped with 3wt.% BCB and sintered at 950 °C.

Table 1. EDX data of 0.95MZCT-0.05CLYT ceramics doped with 3wt.% BCB for areas A-B.

Elements	Mg	Zn	Co	Ti	Ca	La	Y	O
Area A	20.11 (±0.01)	1.23 (±0.02)	1.9 (±0.03)	23.21 (±0.02)	0	0	0	53.55 (±0.02)
Area B	0	0	0	12.75 (±0.01)	9.89 (±0.01)	11.98 (±0.02)	12.1 (±0.01)	53.28 (±0.01)

Figure 4 illustrates the bulk density, relative density, and porosity of 3wt.% BCB-doped xMZCT-(1−x)CLYT ceramics sintered at various temperatures for 4 h. As the temperature rose, the bulk density exhibited an upward trend, reaching a peak value of 3.86 g/cm^3 at 950 °C, after which it gradually declined. The reduction in density is attributed to the abnormal grain growth, as depicted in Figure 2. The variation in permittivity mirrored the density changes, showing an increase with the sintering temperature. Following its zenith at 1150 °C, the permittivity experienced a subsequent decrease. With an increase in sintering temperature, the relative density also increased, as shown in Figure 4b, and the porosity also decreased, as shown in Figure 4c. When the temperature rose to 950 degrees C, the relative density of the xMZCT-(1−x)CLYT ceramics could reach more than 95%, and the porosity reached the minimum value, which was less than 5%.

Figure 5 depicts the permittivity curves of the xMZCT-(1−x)CLYT ceramics at different sintering temperatures over a 4 h period. The relationship between the ε_r values and sintering temperature (presented in Table 2) mirrors the trend observed between density and sintering temperature, given that higher density corresponds to lower porosity. The permittivity exhibited a slight increase with an increase in the sintering temperature. The permittivity of the xMZCT-(1−x)CLYT ceramics showed a progression from 17.27 to 26.2 as the sintering temperature increased from 900 to 950 °C. A peak value of 26.2 was achieved for the 0.85MZCT-0.15CLYT ceramics sintered at 950 °C for 4 h. It is well known that the permittivity of microwave dielectric ceramics is influenced by both the mixing rule and density.

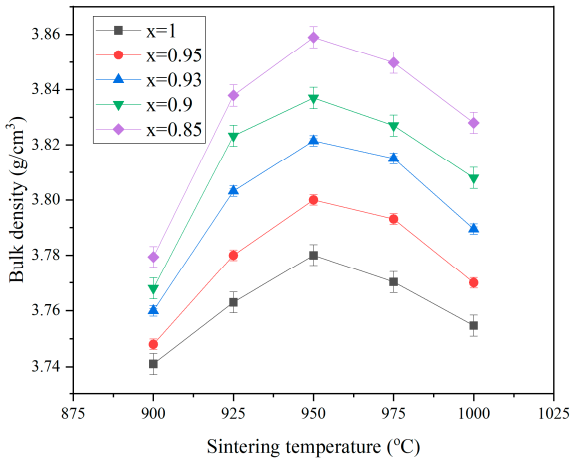

(**a**)

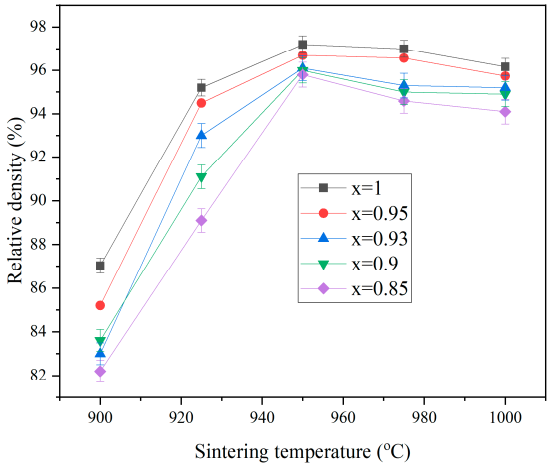

(**b**)

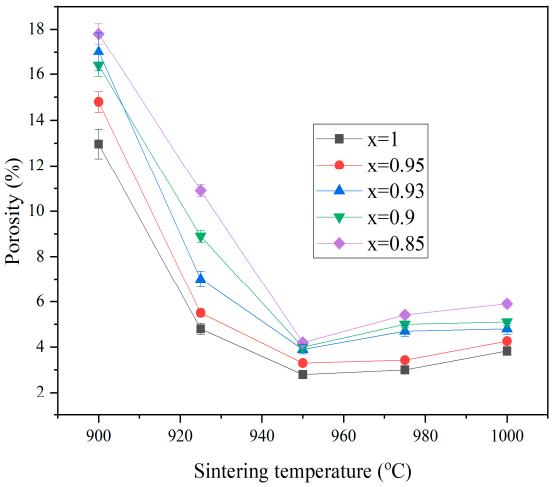

(**c**)

Figure 4. (**a**) Bulk density, (**b**) relative density, and (**c**) porosity of xMZCT-(1-x)CLYT ceramics with 3wt.% BCB as a function of the sintering temperature.

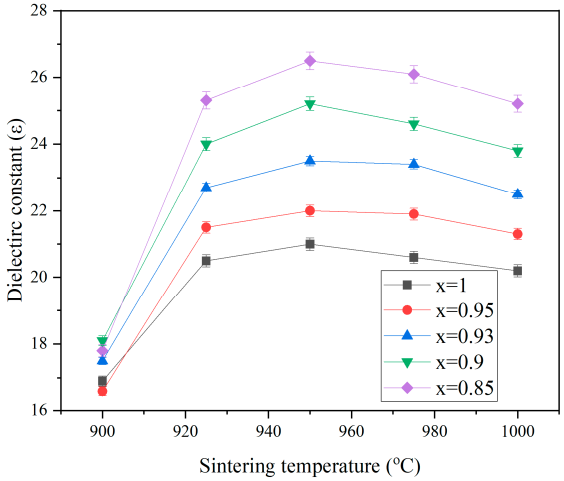

Figure 5. Permittivity curves of xMZCT-(1−x)CLYT ceramics doped with 3wt.% BCB at different sintering temperatures for 4 h.

Table 2. Microwave dielectric properties of the xMZCT-(1-x)CLYT ceramic system doped with 3 wt.% BCB and sintered at 950 °C for 4 h.

x Value	Bulk Density (g/cm^3)	ε_r	Q × f (GHz)	τ_f (ppm/°C)
1	3.78 (±0.04)	20.95 (±0.05)	250,000 (±6700)	−63 (±0.4)
0.95	3.8 (±0.03)	22.5 (±0.01)	190,000 (±3810)	0 (±0.01)
0.93	3.81 (±0.03)	23.5 (±0.02)	180,000 (±1220)	0.1 (±0.05)
0.9	3.83 (±0.02)	25.2 (±0.03)	172,000 (±1800)	10 (±0.3)
0.85	3.88 (±0.03)	26.7 (±0.01)	156,000 (±1610)	21 (±0.5)

It is also known that the permittivity of microwave dielectric ceramics is affected by their ion polarizability. As mentioned above, in xMZCT-(1−x)CLYT, the ε_r value of CLYT increases. To elucidate the effect of CLYT Zn substituting MZCT on the dielectric constant, the ion polarizability of xMZCT-(1−x) CLYT was estimated using the Clausius–Mossotti equation:

$$\varepsilon_r = \frac{3V_m + 8\pi\alpha_m}{3V_m - 4\pi\alpha_m} \quad (2)$$

where ε_r, V_m, and α_m are the relative permittivity, molar volume, and macroscopic polarizability, respectively. Using experimental relative permittivity data and unit cell volume data, the macroscopic polarizability αm was calculated. The theoretical polarizability data in Table 1 show that, with an increase in xMZCT-(1−x)CLYT content, there is almost an S-shaped increase, while the unit cell volume increases with an increase in x. The relative dielectric constant increases as αm increases. When the αm value approaches 3Vm/4π, the relative dielectric constant increases rapidly. It has been reported that the macroscopic polarizability of a complex system with ideal symmetry can be determined by the summation of the polarizabilities of the constituent cations, meaning that:

$$\alpha_m = \Sigma\alpha(\text{ions}) \quad (3)$$

The theoretical polarizability (expressed as αm (theoretical)) value was calculated according to Equation (3). This was compared with the "experimental" polarizability, which was denoted as αm(exp) and determined using the Clausius–Mossotti equation. It should be noted that the αm(exp) of the xMZCT-(1−x)CLYT end member is greater than the αm (theoretical) value, and the αm(exp) value is larger than the αm (theoretical) value. Shannon showed that, as the cation size changes, deviations in the additivity of ion polarizability occur when cation compression or vibration occurs in structural sites. The

lower αm(exp) value of xMZCT-(1−x)CLYT may be due to the compression effect caused by large difference in polarizability MZCT and CLYT ions.

The logarithmic mixing rule, proposed by Lichterecker in 1926, is an intermediate form between serial and parallel mixing [29]:

$$\log \varepsilon_m = v_h \log \varepsilon_h + v_l \log \varepsilon_l \quad (4)$$

where ε_h and ε_l represent the relative permittivity of the high- and dielectric phases, respectively. V_h and V_l denote the volume fractions of the high- and low-dielectric phases, respectively, ensuring that their sum is equal to 1 ($V_h + V_l = 1$). The value ε_m signifies the effective permittivity of the composite.

Microwave dielectric loss primarily arises from factors such as the lattice vibration mode, porosity, secondary-phase impurities and lattice defects. The role of relative density in governing dielectric losses is noteworthy, echoing findings in other microwave dielectric materials. It is widely acknowledged that the factors diminishing the dielectric Q value fall into two categories: natural loss and external loss. Natural loss stems from the interaction between polar phonon vibrations and microwave electric fields in crystals. External loss encompasses phenomena like order–disorder transformations, pore density, grain size, oxygen vacancies, and impurity phases in ceramics. The intrinsic Q value establishes the upper limit for a defect-free single crystal, quantitatively described in the microwave frequency range by the classical damping oscillator model. In this model, under the one-phonon absorption approximation, a reciprocal relationship between Q × f and the permittivity emerges [30]:

$$Q \times f \propto \varepsilon^{-1} \quad (5)$$

where the frequency f is confined within the vicinity of the phonon engine frequency for the validity of the estimation, typically around 10^{12} Hz at room temperature. Nevertheless, a set of experiments has shown that extending the application of Equation (5) from the microwave frequency to the megahertz frequency (1–4 orders of magnitude lower than the optical phonon resonance frequency) at room temperature yields a satisfactory dielectric Q magnitude for well-crafted ceramics. However, the results show that Q × f solely depends on ε_r [30]:

$$Q \times f \propto \varepsilon_r^{-0.6} \quad (6)$$

This implies an inverse relationship between the values of Q × f and ε_r, where, as ε_r increases, Q × f decreases, and vice versa. This phenomenon is most likely attributed to external factors. Numerous authors acknowledge that porosity within a dielectric has an adverse impact on the Q × f values, and the extent of this impact varies depending on the type of dielectric. For low-dielectric Q × f ceramics of the order of 10^3 GHz, the impact of porosity on dielectric Q can be described as $Q = Q_o(1 - 1.5P)$, where Q_o represents the intrinsic dielectric Q measured using microwave reflectance spectroscopy, and P denotes porosity. However, in the case of high Q × f ceramics of the order of 10^5–10^6 GHz, such as polycrystalline Al_2O_3 ceramics, even a small amount of porosity significantly diminishes the dielectric Q, as described by Equation (7) [30,31]:

$$\frac{1}{Q} = (1 - P)\frac{1}{Q_o} + A'P\left(\frac{P}{1 - P}\right)^{2/3} \quad (7)$$

where Qo represents the full-density dielectric quality factor (1.565×10^{-5}), A' is a constant ($=6.3 \times 10^{-3}$), and P is the porosity. Figure 6 illustrates the Q × f value of the xMZCT-(1−x)CLYT ceramics sintered at various temperatures. The Q × f value exhibited an initial increase with rising sintering temperature, reaching a peak value before subsequently declining. Specifically, the peak of the Q × f value was achieved for the xMZCT-(1−x)CLYT ceramics at 950 °C, ranging from 256,000 to 150,000 depending on the value of x. The reduction in the Q × f value is attributed to the abnormal grain growth observed at higher temperatures, as shown in Figure 2.

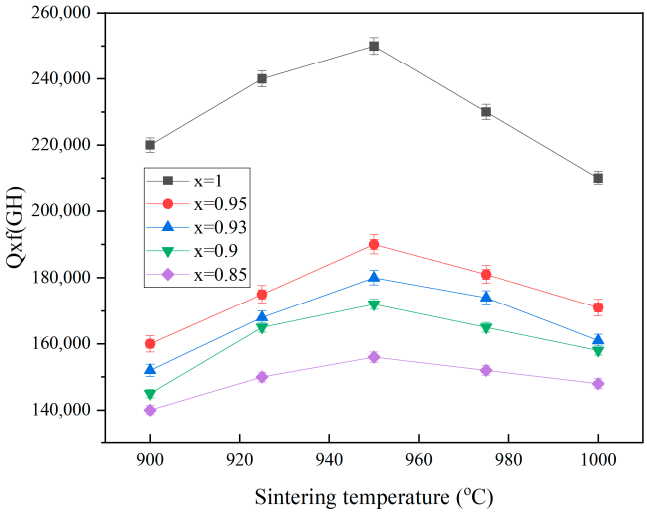

Figure 6. Q × f values of xMZCT-(1−x)CLYT ceramics doped with 3wt.% BCB as a function of the sintering temperature.

The linear thermal expansion coefficient is a fixed parameter in ceramics, and it directly influences the temperature coefficient of capacitance by its correlation with the temperature dependence of the permittivity. The relationship between the temperature coefficient of resonant frequency (τ_f), τ_c, and the thermal expansion coefficient (α_L) is stated in Equation (8) [32]:

$$\tau_f = (\frac{\tau_c}{2} + \alpha_L) \quad (8)$$

Figure 7 illustrates the temperature coefficient of the resonant frequency τ_f for the xMZCT-(1−x)CLYT ceramic system doped with 3wt.% BCB. τ_f is known to be influenced by the composition, additives, and second phase of the material. Given that the τ_f values for MZCT and CLYT are −65 and +320 ppm/°C, respectively, an increase in CLYT content shifts the τ_f value towards a more positive range. This suggests that, by adjusting the amount of CLYT content, a τ_f value of zero can be achieved. A τ_f value of zero was attained with x = 0.95 when sintering was performed at 950 °C for 4 h.

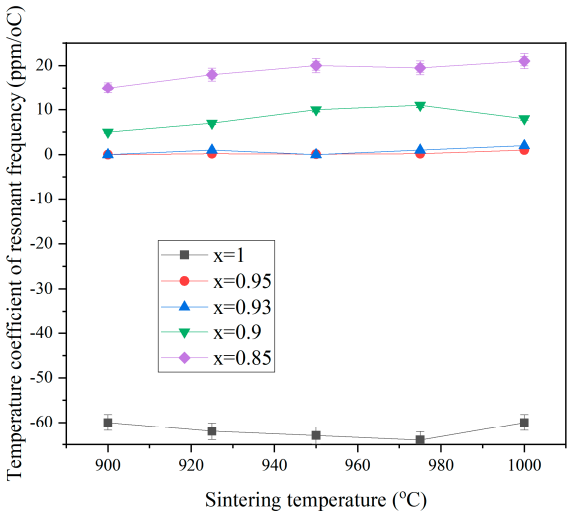

Figure 7. τ_f values of the xMZCT-(1−x)CLYT ceramic system with 3 wt.% BCB sintered at different temperatures for 4 h.

Table 2 presents the microwave dielectric properties of the xMZCT-(1−x)CLYT ceramic system doped with 3 wt.% BCB and sintered at 950 °C for 4 h. As the value of x varied

from 0.95 to 0.85, τ_f underwent a transition from 0 to 21 ppm/°C. The curve exhibited a crossing point at zero, indicating that a τ_f value of zero can be achieved by appropriately adjusting the x value in the xMZCT-(1−x)CLYT ceramic system. However, the Q × f value decreased with decreasing MZCT content, as the CLYT ceramic had a low Q × f value of 23,000 GHz. The microwave dielectric properties of MZCT ceramics were pre-examined, and the findings are elucidated in Table 2. Notably, as the sintering temperature was elevated to 950 °C, significant improvements in key parameters were observed. The measured Q × f reached an impressive 190,000 GHz, indicating an enhanced quality factor and resonant frequency characteristics. Simultaneously, the permittivity (ε_r) exhibited a notable increase, reaching 22.5, showcasing the material's improved response to electric fields. Additionally, the temperature coefficient of resonant frequency (τ_f) was determined to be 0 ppm/°C, highlighting the stability of the ceramics' microwave properties over a range of temperatures. In an effort to refine the microwave dielectric properties of the xMZCT-(1−x)CLYT ceramics, subtle modifications were introduced. Specifically, minute substitutions were made, with Co^{2+} or Zn^{2+} replacing Mg^{2+} to create MZCT, and Y^{3+} taking the place of La^{3+} to form CLYT in the experimental setup.

There may be some uncertainty due to measurement errors in the experiments. These errors, shown in Figures 4–7 and Tables 1 and 2, demonstrate the uncertainty caused by measurement differences.

4. Conclusions

The examination of the microwave properties of the xMZCT-(1−x)CLYT ceramic, doped with 3wt.% BCB, revealed the successful achievement of ultra-low dielectric loss. Specifically, the 0.95MZCT-0.05CLYT ceramic exhibited outstanding microwave properties, even when sintered at low temperatures. This was achieved through the strategic replacement of partial Zn^{2+} and Co^{2+} ions in $MgTiO_3$, resulting in the formation of the $[(Mg_{0.6}Zn_{0.4})_{0.95}Co_{0.05}]_{1.02}$ ceramic. Within the xMZCT-(1−x)CLYT system, a distinctive mix of phases emerged, with MZCT constituting the predominant crystalline phase and CLYT having a minor presence.

This composition displayed strong dielectric properties, featuring a permittivity ε_r of around 20, a noteworthy quality factor (Q × f) that reached 256,000 GHz, and a temperature coefficient of resonant frequency (τ_f) of approximately −65 ppm/°C when sintered at 1200 °C. The intricacies of this composition were further explored at the specific sintering temperature of 950 °C. Under this condition, the system demonstrated exceptional microwave dielectric properties. The ε_r reached 22.5, showing its efficient propagation of electromagnetic waves. The Q × f soared to an impressive 190,000 GHz (measured at 9 GHz), indicating minimal signal loss during transmission. Most notably, the system achieved a τ_f value of zero, implying outstanding temperature stability.

The ultra-low temperature coefficient and high quality factor of the newly discovered 0.95MZCT-0.05CLYT ceramic make it an ideal material for application in the field of 6G band components and GPS antennas. Achieving such good properties at a relatively low sintering temperature aligns with the contemporary drive for energy-efficient and sustainable material processing.

Author Contributions: Conceptualization, Y.-B.C. and J.P.; methodology, Y.-B.C. and J.P.; software, Y.-B.C. All authors have read and agreed to the published version of the manuscript.

Funding: This research received no external funding.

Data Availability Statement: The data presented in this study are available on request from the corresponding author.

Conflicts of Interest: The authors declare no conflict of interest.

References

1. Huang, C.-L.; Wang, J.-J.; Li, B.-J.; Lee, W.-C. Effect of B_2O_3 additives on sintering and microwave dielectric behaviors of 0.66Ca($Mg_{1/3}Nb_{2/3}$)O_3-0.34$CaTiO_3$ ceramics. *J. Alloys Compd.* **2008**, *461*, 440–446. [CrossRef]
2. Huang, C.-L.; Li, G.-J.; Wang, J.-J. Microwave dielectric properties of (1−*x*)($Mg_{0.95}$Zn0.05)TiO3–x(Na0.5La0.5)TiO3 ceramic system. *J. Alloys Compd.* **2009**, *472*, 497–501. [CrossRef]
3. Hsu, C.-H. Improved high-Q microwave dielectric resonator using ZnO-doped La($Co_{1/2}Ti_{1/2}$)O_3 ceramics. *J. Alloys Compd.* **2008**, *464*, 412–417. [CrossRef]
4. Xiao, M.; Sun, H.-R.; Zhou, Z.-Q.; Zhang, P. Bond ionicity lattice energy, bond energy, and microwave dielectric properties of $Ca_{1-x}Sr_xWO_4$ ceramics. *Ceram. Int.* **2018**, *44*, 20686–20691. [CrossRef]
5. Kim, E.-S.; Kim, S.-H.; Lee, B.-I. Low-temperature sintering and microwave dielectric properties of $CaWO_4$ ceramics for LTCC applications. *J. Eur. Ceram. Soc.* **2006**, *26*, 2101–2104. [CrossRef]
6. Krzmanc, M.-M.; Logar, M.; Budic, B.; Suvorov, D. Dielectric and microstructural study of the $SrWO_4$, $BaWO_4$, and $CaWO_4$ scheelite ceramics. *J. Am. Ceram. Soc.* **2011**, *94*, 2464–2472. [CrossRef]
7. Kim, E.S.; Kim, S.H. Effects of structural characteristics on microwave dielectric properties of (1-x)$CaWO_4$-x$LaNbO_4$ ceramics. *J. Electroceram.* **2006**, *17*, 47–77. [CrossRef]
8. Hu, X.-Q.; Jiang, J.; Wang, J.-Z.; Gan, L.; Zhang, T.-J. A new additive-free microwave dielectric ceramic system for LTCC applications: (1-x)$CaWO_4$-x($Li_{0.5}Sm_{0.5}$)WO_4. *J. Mater. Sci. Mater. Electron.* **2020**, *31*, 2544–2550. [CrossRef]
9. Bian, J.-J.; Ding, Y.-M. Structure, sintering behavior, and microwave dielectric properties of (1-x)$CaWO_4$-x$YLiF_4$ (0.02<x<0.10) ceramics. *Mater. Res. Bull.* **2015**, *67*, 245–250.
10. Zhang, S.; Su, H.; Zhang, H.-W.; Jing, Y.-L.; Tang, X.-L. Microwave dielectric properties of $CaWO_4$-Li_2TiO_3 ceramics added with LBSCA glass for LTCC applications. *Ceram. Int.* **2016**, *42*, 15242–15246. [CrossRef]
11. Jeon, C.-J.; Kim, E.-S. Low-temperature sintering of 0.85$CaWO_4$-0.15$LaNbO_4$ ceramics. *Ceram. Int.* **2008**, *34*, 921–924. [CrossRef]
12. Liao, Q.-W.; Wang, Y.-L.; Jiang, F.; Guo, D. Ultra-low fire glass-free $Li_3FeMo_3O_{12}$ microwave dielectric ceramics. *J. Am. Ceram. Soc.* **2014**, *97*, 2394–2396. [CrossRef]
13. Shen, C.-H.; Huang, C.-L. Microwave dielectric properties and sintering behaviors of ($Mg_{0.95}$Ni0.05)TiO3–CaTiO3 ceramic system. *J. Alloys Compd.* **2009**, *472*, 451–455. [CrossRef]
14. Kell, R.C.; Greenham, A.C.; Olds, G.C.E. High-Permittivity Temperature-Stable Ceramic Dielectrics with Low Microwave Loss. *J. Am. Ceram. Soc.* **1973**, *56*, 352–354. [CrossRef]
15. Huanga, C.-L.; Houa, J.L.; Panb, C.-L.; Huang, C.-Y.; Pengd, C.-W.; Weid, C.-H.; Huang, Y.-H. Effect of ZnO additive on sintering behavior and microwave dielectric properties of 0.95MgTiO3-0.05CaTiO3 ceramics. *J. Alloys Compd.* **2008**, *450*, 359–363. [CrossRef]
16. Chen, Y.-C.; Chang, Y.-H. Dielectric properties of B_2O_3-doped La ($Mg_{0.5}Sn_{0.5}$) O_3 ceramics at microwave frequencies. *J. Alloys Compd.* **2009**, *477*, 450–453. [CrossRef]
17. Huang, C.-L.; Chen, Y.-B.; Tasi, C.-F. Influence of V_2O_5 additions to 0.8(Mg0.95Zn0.05)TiO3-0.2Ca0.61Nd0.26TiO3 ceramics on sintering behavior and microwave dielectric properties. *J. Alloys Compd.* **2008**, *454*, 454–459. [CrossRef]
18. Shen, C.-H.; Huang, C.-L. New dielectric material system of $Mg_{0.95}$Co0.05TiO3−Zn0.975Ca0.025TiO3 at microwave frequencies. *J. Alloys Compd.* **2009**, *477*, 712–715.
19. Chen, J.-Y.; Tseng, Y.-W.; Huang, C.-L. Improved high *Q* value of (1−*x*)Ca($Mg_{1/3}Ta_{2/3}$)O_3–*x*$Ca_{0.8}Sm_{0.4/3}TiO_3$ solid solution with zero temperature coefficient of resonant frequency. *J. Alloys Compd.* **2010**, *494*, 205–209. [CrossRef]
20. Cha, H.J.; Kang, D.H.; Cho, Y.S. Dielectric Properties and Crystal Structure of ($Mg_{1-x}Co_x$)2($Ti_{0.95}$Sn0.05)O4 Ceramics. *Mater. Res. Bull.* **2007**, *42*, 265–273. [CrossRef]
21. Wise, P.L.; Reaney, I.M.; Lee, W.E.; Price, T.J.; Iddles, D.M.; Cannell, D.S. Optical Phonon Modes and Dielectric Behavior of $Sr_{1-3x/2}CexTiO_3$ Microwave Ceramics. *J. Eur. Ceram. Soc.* **2001**, *21*, 1723. [CrossRef]
22. Huang, C.-L.; Lin, S.-H.; Liu, S.-S.; Chen, Y.-B. x ($Mg_{0.7}Zn_{0.3}$)$_{0.95}Co_{0.05}TiO_3$-(1−x)($La_{0.5}Na_{0.5}$)TiO_3 ceramic at microwave frequency with a near zero temperature coefficient of resonant frequency. *J. Alloys Compd.* **2010**, *489*, 541–544. [CrossRef]
23. Kim, M.H.; Lim, J.B.; Kim, J.C.; Nahm, S.; Paik, J.H.; Kim, J.H.; Park, K.S. Synthesis of BaCu (B_2O_5) ceramics and their effect on the sintering temperature and microwave dielectric properties of Ba($Zn_{1/3}Nb_{2/3}$)O_3 ceramics. *J. Am. Ceram. Soc.* **2006**, *89*, 3124–3128. [CrossRef]
24. Kim, M.H.; Nahm, S.; Lee, W.-S.; Yoo, M.-J.; Kang, N.-K.; Kim, H.-T.; Lee, H.-J. Effect of B_2O_3 and CuO on the sintering temperature and microwave dielectric properties of Ba($Zn_{1/3}Ta_{2/3}$)O_3 ceramics. *Jpn. J. Appl. Phys.* **2005**, *44*, 3091. [CrossRef]
25. Kim, M.H.; Jeong, Y.H.; Nahm, S.; Kim, H.T.; Lee, H.J. Effect of B_2O_3 and CuO additives on the sintering temperature and microwave dielectric properties of Ba($Zn_{1/3}Nb_{2/3}$)O_3 ceramics. *J. Eur. Ceram. Soc.* **2006**, *26*, 2139. [CrossRef]
26. Zhang, S.; Sahin, H.; Torun, E.; Peeters, F.; Martien, D.; Dilley, N.; Newman, N. Fundamental mechanisms responsible for the temperature coefficient of resonant frequency in microwave dielectric ceramics. *J. Am. Ceram. Soc.* **2017**, *100*, 1508–1516. [CrossRef]
27. Hakki, B.W.; Coleman, P.D. A dielectric resonator method of measuring inductive capacities in the millimeter range. *IEEE Trans. Microw. Theory Tech.* **1960**, *8*, 402. [CrossRef]
28. Courtney, W.E. Analysis and evaluation of a method of measuring the complex permittivity and permeability microwave insulators. *IEEE Trans. Microw. Theory Tech.* **1970**, *18*, 476. [CrossRef]
29. Lichtenecker, K. Die dielektrizitatskonstante naturlicher und kunstlicher mischkorper. *Phys. Z.* **1926**, *27*, 115.

30. Kim, Y.-I.; Woodward, P.M. Crystal structures and dielectric properties of ordered double perovskites containing Mg^{2+} and Ta^{5+}. *J. Solid State Chem.* **2007**, *180*, 2798–2807. [CrossRef]
31. Chen, Y.-B.; Liu, S.-S. Dielectric properties of low Zr-substituted $BaTi_4O_9$ at microwave frequencies. *J. Mater. Sci. Mater. Electron.* **2019**, *30*, 5567–5572. [CrossRef]
32. Reaney, I.M.; Colla, E.L.; Setter, N. Dielectric and Structural Characteristics of Ba- and Sr-based Complex Perovskites as a Function of Tolerance Factor. *Jpn. J. Appl. Phys.* **1994**, *33*, 3984. [CrossRef]

Disclaimer/Publisher's Note: The statements, opinions and data contained in all publications are solely those of the individual author(s) and contributor(s) and not of MDPI and/or the editor(s). MDPI and/or the editor(s) disclaim responsibility for any injury to people or property resulting from any ideas, methods, instructions or products referred to in the content.